



Proceeding Paper

# The Improvement of Methane Plume Detection with High-Resolution Satellite-Based Imaging Spectrometers <sup>†</sup>

Javier Roger <sup>1,\*</sup> , Itziar Irakulis-Loitxate <sup>1,2</sup> , Javier Gorroño <sup>1</sup> , Adriana Valverde <sup>1</sup> and Luis Guanter <sup>1,3</sup>

<sup>1</sup> Research Institute of Water and Environmental Engineering (IIAMA), Universitat Politècnica de València (UPV), 46022 Valencia, Spain

<sup>2</sup> International Methane Emission Observatory (IMEO), United Nations Environment Programme, 75015 Paris, France

<sup>3</sup> Environmental Defense Fund, Reguliersgracht 79, 1017 LN Amsterdam, The Netherlands

\* Correspondence: jarojua@upvnet.upv.es

<sup>†</sup> Presented at the IV Conference on Geomatics Engineering, Madrid, Spain, 6–7 July 2023.

**Abstract:** The detection and monitoring of methane anthropogenic emissions is of vital importance in order to curb global warming. Satellite-based imaging spectrometers, such as PRISMA and EnMAP, have proven instrumental in this task. Methane absorption features from the shortwave infrared spectral range (1000–2400 nm) are exploited by algorithms such as the matched-filter. This method can correctly characterize methane plumes, but retrieval artifacts disturb methane plume detection when using only those spectral channels related to the methane absorption features. Retrievals from simulated plumes and real emission cases from PRISMA and EnMAP data cubes are used to demonstrate that using the whole shortwave infrared region in the matched-filter method results in a better plume detection.

**Keywords:** methane; matched-filter; retrieval; plumes



**Citation:** Roger, J.; Irakulis-Loitxate, I.; Gorroño, J.; Valverde, A.; Guanter, L. The Improvement of Methane Plume Detection with High-Resolution Satellite-Based Imaging Spectrometers. *Environ. Sci. Proc.* **2023**, *28*, 20. <https://doi.org/10.3390/environsciproc2023028020>

Academic Editors: María Belén Benito Oterino, José Fernández Torres, Rosa María García Blanco, Jorge Miguel Gaspar Escribano, Miguel Ángel Manso Callejo and Antonio Vázquez Hoehne

Published: 9 January 2024



**Copyright:** © 2024 by the authors. Licensee MDPI, Basel, Switzerland. This article is an open access article distributed under the terms and conditions of the Creative Commons Attribution (CC BY) license (<https://creativecommons.org/licenses/by/4.0/>).

## 1. Introduction

Methane (CH<sub>4</sub>) plays an important role in slowing global warming in the short to medium term due to its relatively short lifetime in the atmosphere (~10 years) and a global warming potential in the next 20 years almost 100 times greater than carbon dioxide (CO<sub>2</sub>) [1]. Within the range of anthropogenic methane emissions, the coal mining and the oil and gas sectors have been identified as the most efficient sources for reducing emissions. Generally, in these sectors, methane is released from point sources generating concentrated emissions in the form of a plume. Satellite remote sensing has proven to be an optimal tool for the detection of and an optimal tool for detecting and monitoring these plumes, which is key to planning mitigation strategies [2]. In particular, hyperspectral missions such as PRISMA and EnMAP, which use imaging spectroscopy, measure solar radiation reflected by the earth in the 400–2500 nm spectral range, where there are absorption windows that allow methane to be characterized. One of the most commonly used methods to detect plumes in imaging spectroscopy is the matched-filter. Although this method allows us to characterize methane emissions, some area structures are erroneously confused for methane in the methane concentration maps, which makes plume detection difficult. In this work, we will exploit the spectral range of application of the matched-filter method in order to improve plume detection. In this context, we will also investigate whether there is an improvement in methane plume quantification.

## 2. Materials and Methods

### 2.1. Materials

In this work, we have used 2 L1B and 1 L1 data cubes from the EnMAP and PRISMA missions, respectively. From EnMAP, we use a data cube from the Hassi Messaoud oil and

gas field in Algeria (lat, lon = 31.782, 5.960) and other close to the Apex landfill location in Nevada, U.S. (lat, lon = 36.386, -114.907). From PRISMA, we use a data cube from a coal mine site in the city of Shanxi in China (lat, lon = 37.828, 113.715).

## 2.2. Matched-Filter Method

In order to retrieve methane concentration maps, we use the matched-filter method. This algorithm models the data cube as a multivariate Gaussian distribution and assumes area homogeneity and methane sparsity. Those pixels more distant from the mean spectrum whose difference can be related to methane absorption will obtain a higher methane concentration enhancement value, i.e., concentration in reference to the background levels. Satellite-based imaging spectrometers operate in the visible and near Infrared (VNIR: 400–1000 nm) and in the shortwave Infrared (SWIR: 1000–2400 nm) spectra. From the latter, a weak and a strong absorption window can be found around 1700 nm and 2300 nm, respectively. In the bibliography, the matched-filter applied in the 2300 nm window spectral range (2300-MF) is extensively used [3,4]. However, when using 2300-MF, we can usually find structures that erroneously score as methane emissions in the methane concentration maps. This leads to the existence of false positives and other retrieval artifacts that complexify the plume detection capability. One of the causes that can lead to retrieval artifacts is the similarity of the related structures to methane spectral absorption features. In order to deal with these retrieval artifacts, we change the spectral range of application of the matched-filter to the whole SWIR spectrum (SWIR-MF). Structures overlapping with methane absorption features at the 2300 nm window could present other features along the SWIR spectrum that methane does not. Therefore, because of a more stringent spectrum to match, SWIR-MF would attenuate or practically remove retrieval artifacts. Additionally, the more demanding spectrum will generally attenuate the retrieval values. Consequently, those pixels with higher values in the SWIR-MF will be changed to their 2300-MF values to avoid new disturbing enhancements. Because of the retrieval attenuation, we will show methane concentration maps in the range of values from 0 to 3 times its standard deviation ( $\sigma$ ). In this manner, we can compare the relative contrast between the methane emissions and the background to assess the plume detection capability.

## 2.3. Quantification and Detection of Methane Emissions

We also assess the quantification capability of 2300-MF and SWIR-MF with simulated plumes. These are generated by large-eddy simulations with the weather and research forecasting model (WRF-LES) [5] adapted to the spatial sampling of our data. We calculate the total excess of methane mass of the plume with the IME (kg) magnitude as in Frankenberg et al. [6] for both spectral ranges, and compare to the IME of reference ( $IME_{ref}$ ). Additionally, a methane emission is detected when it originates from a potential source and aligns to wind direction. We check the former with radiance bands from the data cube and high spatial resolution images (e.g., Google Earth) and the latter from the GEOS-FP [7].

## 3. Results

### 3.1. End-to-End Simulation Analysis

In Figure 1, we can observe the methane retrievals of the 2300-MF (top-left) and the SWIR-MF combined with the 2300-MF (top-right) where a simulated plume (at the center of each retrieval) was implemented in a data cube in a Nevada site. We can observe that in the 2300-MF, there is a pronounced retrieval artifact that comes from solar panels, but in the combined matched-filter this is practically removed. Additionally, background noise around the plume is attenuated because of the combination of both retrievals.

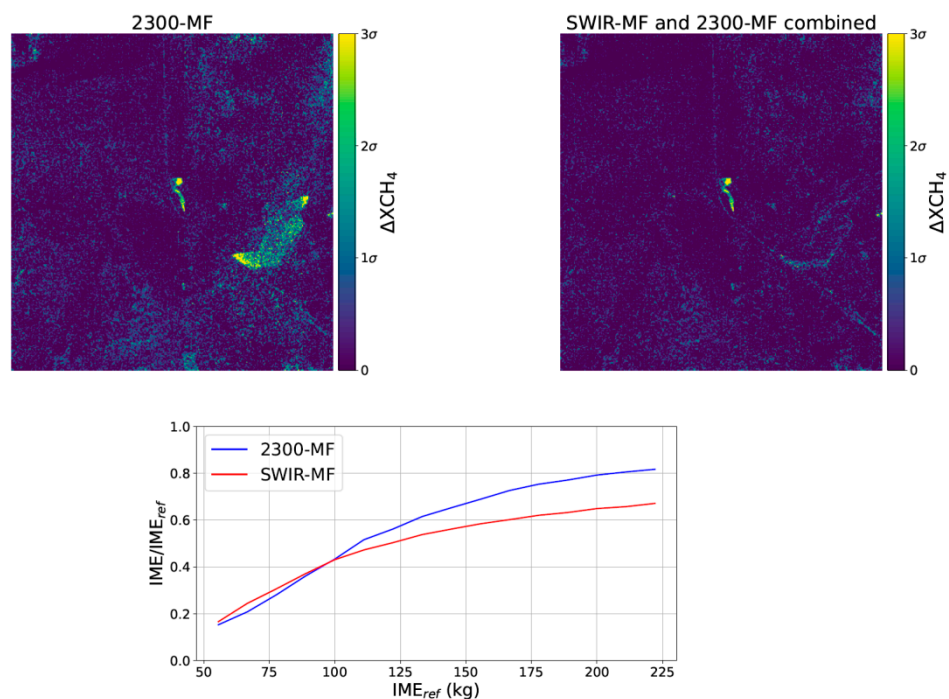


**Figure 1.** Methane retrieval using 2300-MF (**top-left**) and the combined matched-filter (**top-right**) from an EnMAP data cube in Nevada with a simulated plume, and the reference IME ( $IME_{ref}$ ) vs. the calculated IME from the 2300-MF (blue) and the SWIR-MF (red) divided by  $IME_{ref}$  (**bottom**).

In Figure 1, we also show the comparison between the quantification for the 2300-MF and SWIR-MF method (bottom). We see that at low IME values, both are distanced from the  $IME_{ref}$ . This is because we are under the detection limit, and it is difficult to characterize the plume. However, at higher IME values, 2300-MF becomes closer to the  $IME_{ref}$  in reference to SWIR-MF.

### 3.2. Real Cases

In Figure 2 are real cases of methane emissions with the 2300-MF and the SWIR-MF combined in an oil and gas site in Argelia, coming from a potential emitting facility and in a coal mine site in China from a venting shaft. Both plumes are located at center of each panel, and follow an easterly direction that was confirmed with GEOS-FP data.

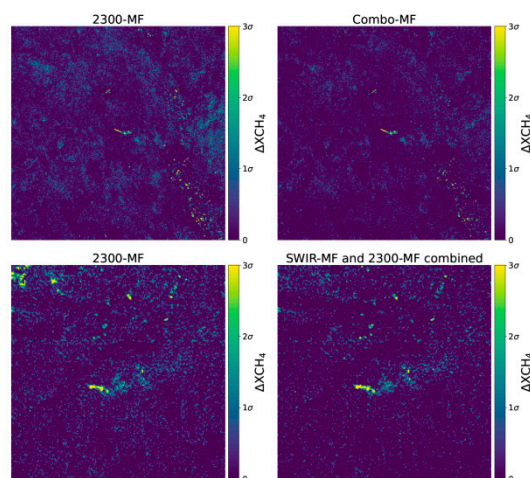


**Figure 2.** Methane retrieval using 2300-MF (**left**) and the combined matched-filter (**right**) from an EnMAP data cube in Argelia (**top**) and from a PRISMA data cube in China (**bottom**).

For the combined matched-filter applied in the Argelia site data cube, we can see a subtle attenuation in retrieval artifacts coming from oil and gas facilities and a major reduction in background noise. On the other hand, in the China site, retrieval artifacts coming from an urban area are practically removed, and there is also a substantial reduction in background noise.

#### 4. Conclusions

The matched-filter applied to the whole SWIR spectral range combined with the matched-filter applied to the 2300 nm methane absorption window is able to reduce background noise and attenuate retrieval artifacts, which improves methane plume detection. However, the quantification of the methane plume is better preserved with the matched-filter applied to the 2300 nm window.

**Author Contributions:** Conceptualization, J.R.; methodology, J.R.; formal analysis, J.R.; investigation, J.R.; resources, J.R. and I.I.-L.; writing—original draft preparation, J.R.; writing—review and editing, J.R., I.I.-L., J.G., A.V. and L.G.; supervision, L.G. All authors have read and agreed to the published version of the manuscript.

**Funding:** This study was funded by the HiResCH4 SA Contract 4000135294/21/I-DT-Ir CCN, FUTURE EO-1 EO SCIENCE FOR SOCIETY PERMANENTLY OPEN CALL FOR PROPOSALS. Project web: <https://hiresch4.upv.es/> (accessed on 13 April 2023).

**Acknowledgments:** The authors thank the Italian Space Agency and the DLR Space Agency for the PRISMA and EnMAP data used in this work, respectively.

**Conflicts of Interest:** One of the authors, I.I.-L., is affiliated with the United Nations. Similarly, another author, L.G., is affiliated with the Environmental Defense Fund.

#### References

1. IPCC. *Climate Change 2013: The Physical Science Basis. Contribution of Working Group I to the Fifth Assessment Report of the Intergovernmental Panel on Climate Change*; Stocker, T.F., Qin, D., Plattner, G.-K., Tignor, M., Allen, S.K., Boschung, J., Nauels, A., Xia, Y., Bex, V., Midgley, P.M., Eds.; Cambridge University Press: Cambridge, UK, 2013.
2. Irakulis-Loitxate, I.; Guanter, L.; Liu, Y.-N.; Varon, D.J.; Maasackers, J.D.; Zhang, Y.; Chulakadabba, A.; Wofsy, S.C.; Thorpe, A.K.; Duren, R.M.; et al. Satellite-based survey of extreme methane emissions in the Permian basin. *Sci. Adv.* **2021**, *7*, eabf4507. [[CrossRef](#)] [[PubMed](#)]
3. Foote, M.D.; Dennison, P.E.; Thorpe, A.K.; Thompson, D.R.; Jongaramrungruang, S.; Frankenberg, C.; Joshi, S.C. Fast and Accurate Retrieval of Methane Concentration from Imaging Spectrometer Data Using Sparsity Prior. *IEEE Trans. Geosci. Remote. Sens.* **2020**, *58*, 6480–6492. [[CrossRef](#)]
4. Thompson, D.R.; Leifer, I.; Bovensmann, H.; Eastwood, M.; Fladeland, M.; Frankenberg, C.; Gerilowski, K.; Green, R.O.; Kratwurst, S.; Krings, T.; et al. Real-time remote detection and measurement for airborne imaging spectroscopy: A case study with methane. *Atmospheric Meas. Tech.* **2015**, *8*, 4383–4397. [[CrossRef](#)]
5. Varon, D.J.; Jacob, D.J.; McKeever, J.; Jervis, D.; Durak, B.O.A.; Xia, Y.; Huang, Y. Quantifying methane point sources from fine-scale satellite observations of atmospheric methane plumes. *Atmos. Meas. Tech.* **2018**, *11*, 5673–5686. [[CrossRef](#)]
6. Frankenberg, C.; Thorpe, A.K.; Thompson, D.R.; Hulley, G.; Kort, E.A.; Vance, N.; Borchardt, J.; Krings, T.; Gerilowski, K.; Sweeney, C.; et al. Airborne methane remote measurements reveal heavy-tail flux distribution in Four Corners region. *Proc. Natl. Acad. Sci. USA* **2016**, *113*, 9734–9739. [[CrossRef](#)] [[PubMed](#)]
7. Molod, A.; Takacs, L.; Suarez, M.; Bacmeister, J.; Song, I.-S.; Eichmann, A. *The GEOS-5 Atmospheric General Circulation Model: Mean Climate and Development from MERRA to Fortuna. Technical Memorandum (TM)*; NASA Technical Report Series on Global Modeling and Data Assimilation; NASA: Greenbelt, MD, USA, 2012; NASA TM—2012-104606.

**Disclaimer/Publisher's Note:** The statements, opinions and data contained in all publications are solely those of the individual author(s) and contributor(s) and not of MDPI and/or the editor(s). MDPI and/or the editor(s) disclaim responsibility for any injury to people or property resulting from any ideas, methods, instructions or products referred to in the content.